

## Magnetoreflexion in Bismuth

RICHARD N. BROWN,<sup>†</sup> JOHN G. MAVROIDES

*Lincoln Laboratory,\* Massachusetts Institute of Technology, Lexington, Massachusetts*

AND

BENJAMIN LAX

*Lincoln Laboratory,\* Massachusetts Institute of Technology, Lexington, Massachusetts*

and

*National Magnet Laboratory,\*\* Massachusetts Institute of Technology, Cambridge, Massachusetts*

Direct interband transitions have been observed in the infrared magnetoreflexion of single-crystal bismuth at low temperatures. They are manifested by oscillations which are almost periodic in  $1/H$ . Analysis in terms of a two-band model yields the energy gap,  $\epsilon_g = 0.015 \pm 0.002$  eV, and also the cyclotron masses at the bottom of the conduction band for two orientations of the magnetic field with respect to the crystallographic axes. Within the resolution of the instrument, the  $g$  factors of the conduction and valence bands are equal.

### INTRODUCTION

OSCILLATIONS in the magnetoreflexion of bismuth were first observed by Keyes *et al.*<sup>1</sup> Their results indicated that the conduction band was non-quadratic. Boyle and Rodgers<sup>2</sup> subsequently observed oscillations in transmission, and found a band edge in the vicinity of  $20 \mu$ . They interpreted this edge as the onset of direct transitions to the conduction band from a lower lying band. Lax<sup>3-5</sup> proposed a model which explained the nonquadratic behavior of the conduction band in terms of interaction with this lower lying band. This model has also been considered by Wolff.<sup>6</sup> On theoretical grounds, Cohen<sup>7</sup> and Lax<sup>5</sup> later pointed out the need for a modification of the model, and Cohen presented more detailed dispersion relations.

These developments suggested the possibility of observing direct transitions in a magnetic field between Landau levels in the lower band and the conduction band. These transitions were observed in preliminary measurements<sup>8</sup> with the magnetic field parallel to the surface of the sample. This paper reports more extensive measurements with the magnetic field normal to the surface of the sample. The measurements have been extended to higher magnetic fields and longer wavelengths. New results include the observation of the lowest interband transition, as well as the magneto-plasma effect.

<sup>†</sup> Present address National Magnet Laboratory.

\*Operated with support from the U. S. Army, Navy, and Air Force.

\*\* Supported by the Air Force Office of Scientific Research.

<sup>1</sup> R. J. Keyes, S. Zwerdling, S. Foner, H. H. Kolm, and B. Lax, *Phys. Rev.* **104**, 1804 (1956).

<sup>2</sup> W. S. Boyle and K. F. Rodgers, *Phys. Rev. Letters* **2**, 338 (1959).

<sup>3</sup> B. Lax, *Bull. Am. Phys. Soc.* **5**, 167 (1960).

<sup>4</sup> B. Lax, J. G. Mavroides, H. J. Zeiger, and R. J. Keyes, *Phys. Rev. Letters* **5**, 241 (1960).

<sup>5</sup> B. Lax and J. G. Mavroides, in *Advances in Solid State Physics*, edited by F. Seitz and D. Turnbull (Academic Press Inc., New York, 1960), Vol. 11; B. Lax, *The Fermi Surface*, edited by W. A. Harrison and M. B. Webb (John Wiley & Sons, Inc., New York, 1960).

<sup>6</sup> P. A. Wolff (to be published).

<sup>7</sup> M. H. Cohen, *Phys. Rev.* **121**, 387 (1961).

<sup>8</sup> R. N. Brown, J. G. Mavroides, M. S. Dresselhaus, and B. Lax, *Phys. Rev. Letters* **5**, 243 (1960).

### EXPERIMENTAL

The apparatus is shown in Fig. 1. The reflection spectra were obtained by shining a monochromatic infrared beam onto an electropolished surface of single-crystal bismuth<sup>9</sup> at nearly normal incidence. A Perkin-Elmer monochromator was employed with suitable prisms to cover the photon energy range from 0.040 to 0.200 eV. The reflected beam was detected by a thermocouple. The sample was mounted on a copper block which was in contact with liquid helium or liquid nitrogen. Because of this, the temperature of the sample was probably a few degrees higher than that of the liquid. The Dewar was placed in a 2-in.-bore solenoid magnet. The focal length of the beam produced by the monochromator was increased with the use of paraboloids, in order to fit the beam into the rather small aperture presented by the magnet.

The samples were oriented by x-ray techniques, such that the magnetic field was along either a binary or a bisectrix axis. The field was normal to the surface from which the infrared beam was reflected. The field was swept continuously from zero to a maximum, and back to zero, usually with a period of 12 min.

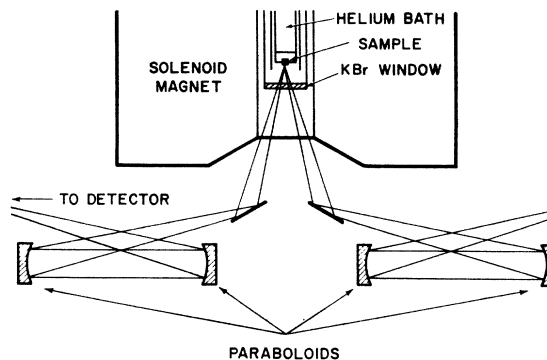


FIG. 1. Apparatus. Magnet and Dewar are shown in cross section.

<sup>9</sup> The samples were obtained from single-crystal bismuth of 99.9999% purity, which was grown by S. Fischler of Lincoln Laboratory by pulling from the melt.

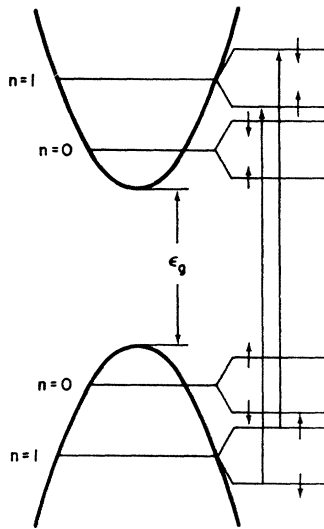


FIG. 2. Energy bands in a magnetic field showing Landau levels and spin splitting.

**THEORETICAL**

According to Lax's model the energy levels in a magnetic field can be written

$$\epsilon = -\frac{1}{2}\epsilon_g \pm \frac{1}{2}[\epsilon_g^2 + 4\epsilon_g(n + \frac{1}{2} + m)\beta_0^*H]^{1/2}, \quad (1)$$

where the plus sign is taken for the conduction band, and the minus sign for the valence band. Here  $\epsilon_g$  is the vertical energy gap between the two bands,  $\beta_0^* = e\hbar/m_0^*c$ , and  $m_0^*$  is the cyclotron effective mass at the bottom of the conduction band. In the following we assume that the spin splitting is equal to the Landau spacing ( $m = \pm \frac{1}{2}$ ), according to Cohen and Blount.<sup>10</sup> The energy bands and Landau levels are shown in Fig. 2. The ordinary interband selection rules for the configuration of this experiment are  $\Delta n = 0$ ,  $\Delta m = \pm 1$ , where  $m$  is the total angular momentum quantum number. Accordingly, the photon energy is

$$\epsilon_p = \frac{1}{2}[\epsilon_g^2 + 4\epsilon_g(n+1)\beta_0^*H]^{1/2} + \frac{1}{2}(\epsilon_g^2 + 4\epsilon_g n\beta_0^*H)^{1/2}. \quad (2)$$

From Eq. (2) it follows that

$$\frac{1}{H} = \frac{\epsilon_g\beta_0^*}{(\epsilon_p^2 - \epsilon_g^2)} \left\{ 2n + 1 + \left[ 4n(n+1) + \frac{\epsilon_g^2}{\epsilon_p^2} \right]^{1/2} \right\}. \quad (3)$$

If  $\epsilon_p > \epsilon_g$ , then, for  $n \geq 1$ , Eq. (3) becomes

$$1/H \approx [\epsilon_g\beta_0^*/(\epsilon_p^2 - \epsilon_g^2)]4(n + \frac{1}{2}). \quad (4)$$

Therefore, the transitions are almost periodic in  $1/H$ , with a period

$$\Delta = 4\epsilon_g\beta_0^*/(\epsilon_p^2 - \epsilon_g^2). \quad (5)$$

The  $n=0$  transition does not obey Eq. (4), but from Eq. (3) we find

$$\frac{1}{H_0} = \frac{\epsilon_g\beta_0^*}{(\epsilon_p^2 - \epsilon_g^2)} \left( 1 + \frac{\epsilon_g}{\epsilon_p} \right) = \frac{\beta_0^*}{(\epsilon_p - \epsilon_g)} \left( \frac{\epsilon_g}{\epsilon_p} \right). \quad (6)$$

<sup>10</sup> M. H. Cohen and E. I. Blount, *Phil. Mag.* **5**, 115 (1960).

According to Eq. (4), a plot of reciprocal fields vs integers should yield a straight line with a slope given by Eq. (5), and an intercept,  $n = -\frac{1}{2}$ . Then Eq. (5) tells us that a plot of reciprocal periods versus  $\epsilon_p^2$  should yield a straight line with slope

$$\frac{1}{4\epsilon_g\beta_0^*} = \frac{c}{4e\hbar} \left( \frac{m_0^*}{\epsilon_g} \right). \quad (7)$$

From Eq. (6) we may obtain an expression for the apparent mass of the  $n=0$  line, defined by

$$m_a = (e\hbar/c)(H/\epsilon_p). \quad (8)$$

The result is

$$m_a = (m_0^*/\epsilon_g)(\epsilon_p - \epsilon_g), \quad (9)$$

which indicates that a plot of  $m_a$  vs  $\epsilon_p$  should yield a straight line with slope,  $m_0^*/\epsilon_g$ .

Since a transition proceeds from an occupied to an unoccupied state, the transition will not occur, unless the final state is above the Fermi level. The  $n$ th Landau level in the conduction band passes through the Fermi level at a field determined by Eq. (1), where we set  $\epsilon = \epsilon_f$ .

$$\epsilon_f = -\frac{1}{2}\epsilon_g + \frac{1}{2}[\epsilon_g^2 + 4(n+1)\epsilon_g\beta_0^*H]^{1/2}. \quad (10)$$

If we insert this field value into Eq. (2), we obtain the cutoff energy, below which the transition will not be observed.

$$\epsilon_{p \text{ min}} = \frac{1}{2}(2\epsilon_f + \epsilon_g) + \frac{1}{2}[\epsilon_g^2 + (n/n+1)[(2\epsilon_f + \epsilon_g)^2 - \epsilon_g^2]]^{1/2}. \quad (11)$$

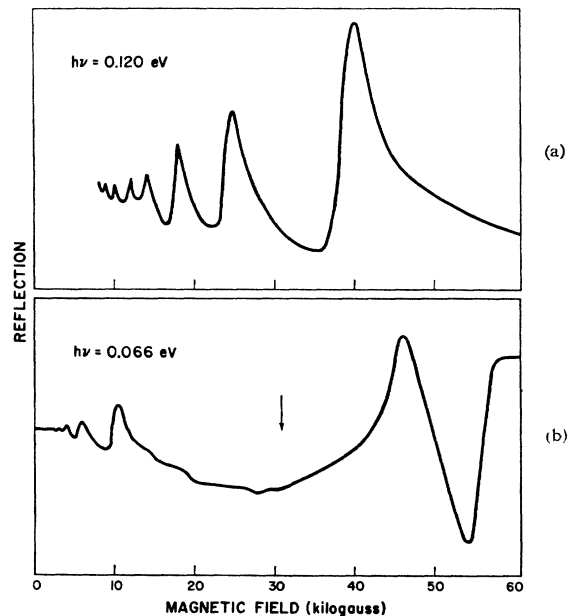


FIG. 3. Typical recorder traces with the magnetic field along a binary axis and  $T = 4.2^\circ\text{K}$ . Part (a) is at a photon energy of 0.120 eV, and part (b) is at 0.066 eV.

For large  $n$ , Eq. (11) reduces to

$$\epsilon_{p \text{ min}} \approx 2\epsilon_f + \epsilon_g, \quad (12)$$

while for  $n=0$ , we have

$$\epsilon_{p \text{ min}} = \epsilon_f + \epsilon_g. \quad (13)$$

From Eq. (1) we may also obtain the photon energies of the intraband or cyclotron resonance transitions for which the selection rules are  $\Delta n = 1$ ,  $\Delta m = 0$ ,

$$\epsilon_p = \frac{1}{2} [\epsilon_g^2 + 4\epsilon_g(n + \frac{1}{2} + m)\beta_0^* H]^{1/2} - \frac{1}{2} [\epsilon_g^2 + 4\epsilon_g(n - \frac{1}{2} + m)\beta_0^* H]^{1/2}. \quad (14)$$

Only one transition will be observed in a given range of magnetic fields corresponding to the  $n$ th Landau level below the Fermi level, and the  $(n+1)$ st above.

$$\frac{1}{(n+1)} \frac{\epsilon_f(\epsilon_f + \epsilon_g)}{\epsilon_g \beta_0^*} < H < \frac{1}{n} \frac{\epsilon_f(\epsilon_f + \epsilon_g)}{\epsilon_g \beta_0^*}. \quad (15)$$

Near a plasma edge the cyclotron resonance will appear shifted according to<sup>5</sup>

$$\epsilon_p' = \frac{1}{2} \epsilon_p + \frac{1}{2} (\epsilon_p^2 + 4\epsilon_{pl}^2)^{1/2}, \quad (16)$$

where  $\epsilon_{pl}$  is the plasma energy.

According to the tilted-ellipsoid model of Shoenberg<sup>11</sup> the effective cyclotron mass,  $m_0^*$ , is given, in terms of the component masses, as follows.<sup>12</sup>

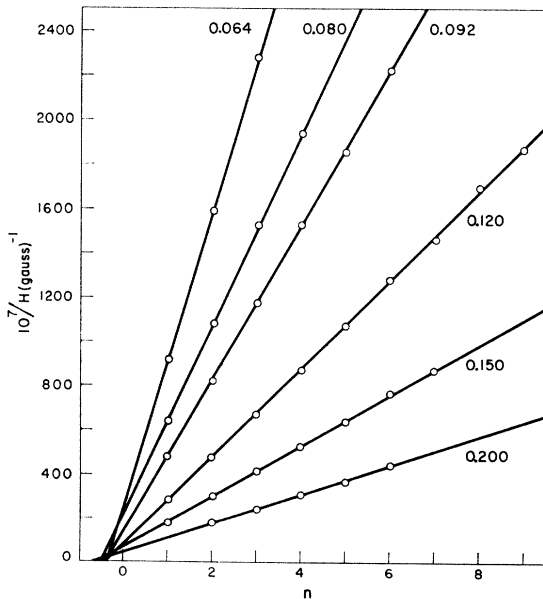


FIG. 4. Reciprocal magnetic fields versus integers with  $H$  along a binary axis. The photon energy is indicated on each line.

<sup>11</sup> D. Shoenberg, Proc. Roy. Soc. (London) **A170**, 341 (1939).

<sup>12</sup> B. Lax, K. J. Button, H. J. Zeiger, and L. M. Roth, Phys. Rev. **102**, 715 (1956).

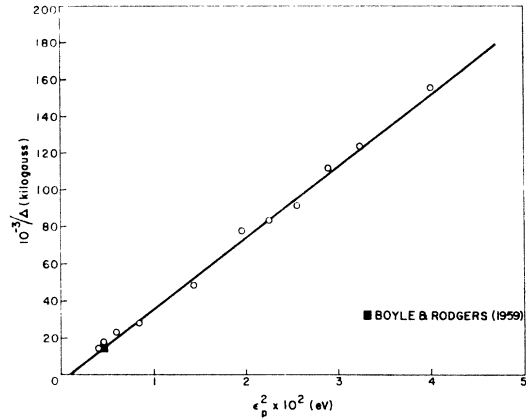


FIG. 5. Reciprocal periods versus the square of the photon energy with  $H$  along a binary axis.

$H \parallel$  binary:

$$(m_0^*)_a = m_0(m_2 m_3 - m_4^2)^{1/2},$$

$$(m_0^*)_b = (m_0^*)_c = 2m_0 \left[ \frac{m_1(m_2 m_3 - m_4^2)}{m_1 + 3m_2} \right]^{1/2}.$$

$H \parallel$  bisectrix:

$$(m_0^*)_a = m_0 [(m_2 m_3 - m_4^2) m_1 / m_2]^{1/2},$$

$$(m_0^*)_b = (m_0^*)_c = 2m_0 \left[ \frac{m_1(m_2 m_3 - m_4^2)}{3m_1 + m_2} \right]^{1/2}. \quad (17)$$

Here axes 1, 2, and 3 refer to the binary, bisectrix, and trigonal, respectively.

## RESULTS

### A. $H \parallel$ Binary

Figure 3 is a reproduction of two recorder traces with the magnetic field along a binary axis. Part (a) of Fig. 3 was obtained at a photon energy of 0.120 eV, and shows transitions  $n=1$  to  $n=7$ . Part (b), obtained at a photon energy of 0.066 eV, shows the  $n=0$  transition at  $H=46.2$  kG, and the plasma line at higher fields. The arrow indicates the field at which the peak of the  $n=0$  transition would occur, if the transitions were strictly periodic in  $1/H$ . The field value corresponding to a transition is read at the peak of the oscillation.<sup>13</sup> Figure 4 is a plot of reciprocal fields versus integers for several photon energies. The period is obtained from the slope of the straight line. Reciprocal periods are plotted in Fig. 5 vs the square of the photon energy. From the slope of this line we evaluate  $m_0^*/\epsilon_g$ , according to Eqs. (5) and (7). Figure 6 is a plot of the apparent mass of the  $n=0$  line vs the photon energy, which, according to Eq. (9), yields an additional value of the parameter,  $m_0^*/\epsilon_g$ . Figure 7 is a plot of photon energy versus magnetic field, where the data are represented by circles, and the curves are obtained from Eq. (2). We have

<sup>13</sup> M. S. Dresselhaus and G. Dresselhaus, Phys. Rev. **125**, 499 (1962).

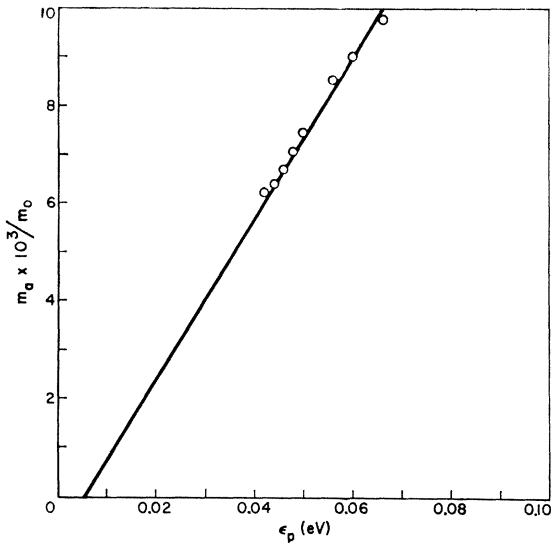


FIG. 6. Apparent mass of the  $n=0$  line, defined by Eq. (8), versus the photon energy, with  $H$  along a binary axis.

inserted into Eq. (2) the values of  $m_0^*/\epsilon_g$  and  $\epsilon_g$  which gave the best fit. They are listed in Table I.

**B.  $H \parallel$  Bisectrix**

Figures 8–12 show the same type of analysis as above, but with the field along a bisectrix axis. Here we see two sets of transitions, one set weaker than the other. The weaker sets corresponds to the heavier mass associated with two of the ellipsoids.

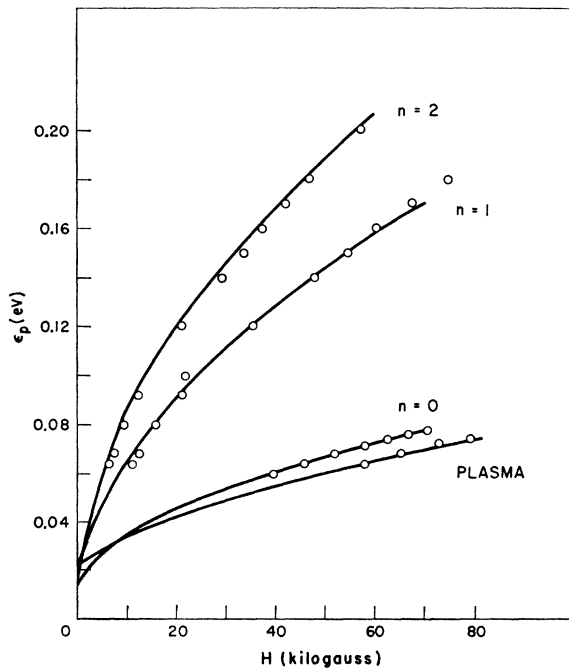


FIG. 7. Photon energies versus magnetic field and  $H$  along a binary. Solid curves are obtained from Eq. (2).

TABLE I. Values of the parameters of the theoretical model. The energy gap,  $\epsilon_g$ , is quoted in eV. The uncertainty in  $m_0^*$  is  $\pm 40\%$ .

	$(\epsilon_g/m_0^*)m_0$			$\epsilon_g$	$m_0^*/m_0$
	Figs. 5 and 10	Figs. 6 and 11	Figs. 7 and 12		
$H \parallel$ binary	5.6	6.1	6.1	0.015	0.00246
$H \parallel$ bisectrix					
(a) light mass	6.6	7.3	7.1	0.015	0.00212
(b) heavy mass	2.9		3.3	0.015	0.00455

**DISCUSSION**

We believe that the simplicity of the spectrum which we have observed implies that the  $g$  factors of the conduction and valence bands are essentially equal. This can be seen by referring to Fig. 2. Here some of the orbital degeneracy of the levels is shown removed by the large  $g$  factor,<sup>14</sup> so that each level is split into two levels. Now there are two transitions of the type  $\Delta n=0$ ,  $\Delta m=\pm 1$  for each  $n$ , namely,  $\Delta m=+1$  and  $\Delta m=-1$ , as shown by the arrows for  $n=1$ . Clearly, if the  $g$  factors were significantly different, these two transitions would occur at different photon energies for the same magnetic field, or at different fields for the same energy, and the spectrum would not be simply periodic.

Further evidence in support of this claim is given by the intercept in Figs. 4 and 9. Aside from scatter in the data, the value appears to be  $n = -\frac{1}{2}$ , in agreement with Eq. (4). We cannot easily generalize Eq. (2), in order to show the implication of this intercept, but if we write the photon energy as follows:

$$\epsilon_p = \epsilon_g + (n + \frac{1}{2} \pm \Delta_c)\beta_c H + (n + \frac{1}{2} \mp \Delta_v)\beta_v H, \quad (18)$$

where  $c$  and  $v$  refer to the conduction and valence bands, respectively, we find

$$\frac{1}{H} = \frac{(n + \frac{1}{2})(\beta_c + \beta_v) \pm (\Delta_c \beta_c - \Delta_v \beta_v)}{\epsilon_p - \epsilon_g}. \quad (19)$$

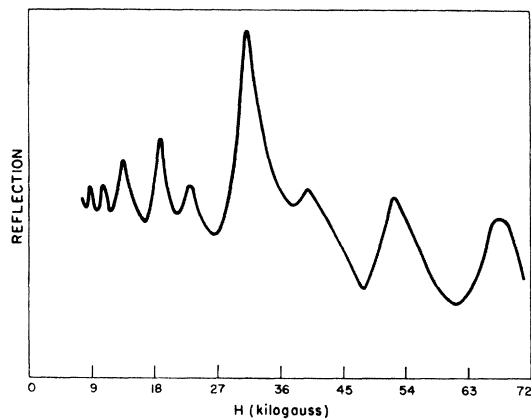
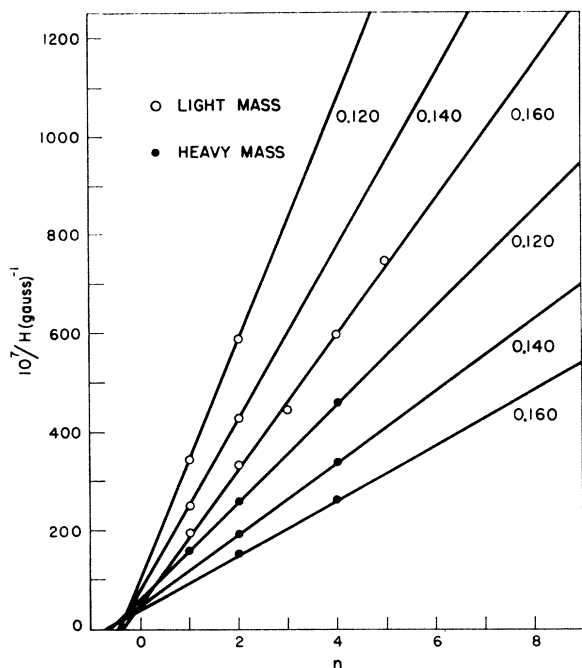


FIG. 8. A typical recorder trace with  $H$  along a bisectrix axis. The photon energy is 0.120 eV and  $T=4.2^\circ\text{K}$ .

<sup>14</sup> G. E. Smith, J. K. Galt, and F. R. Merritt, Phys. Rev. Letters 4, 276 (1960).


 FIG. 9. Reciprocal fields versus integers with  $H$  along a bisectrix.

Now an intercept near  $n = -\frac{1}{2}$  implies

$$\Delta\alpha\beta_c - \Delta\alpha\beta_v \approx 0, \quad (20)$$

which may be written

$$g_c - g_v \approx 0, \quad (21)$$

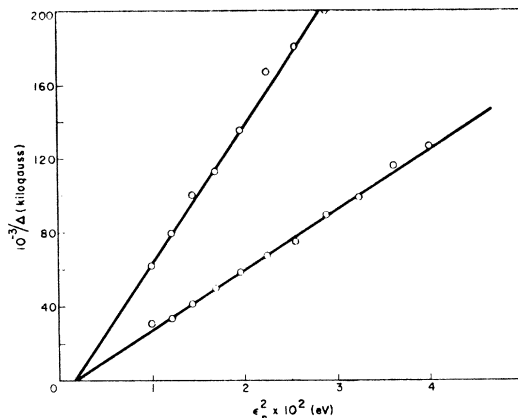
since  $\Delta\alpha\beta_c = \frac{1}{2}g_c(e\hbar/2m_0c)$ . From the resolution of the instrument, we estimate  $|g_c - g_v| < 12$ .

The result of fitting Lax's model to the data is a set of values of the energy gap and the cyclotron mass at the bottom of the band. The actual analysis yields the ratio of the gap to the mass,  $\epsilon_g/m_0^*$ , and the gap,  $\epsilon_g$ , from which the mass is deduced. It will be noted that the analysis of the higher transitions,  $n > 0$ , differs from the analysis of the  $n = 0$  transition. The former does not yield a reliable value of  $\epsilon_g$ , since the magnetic energy is large compared to the gap. This is not the case, however, for the  $n = 0$  transition, where it is found that the curves of  $\epsilon_p$  versus  $H$  are sensitive to the gap, so that a reliable value is obtained by curve fitting. This value is  $\epsilon_g = 0.015 \pm 0.002$  eV. In addition, the separation of the  $n = 0$  transition from the plasma line is found to be sensitive to the gap. In fact, the ratio of the magnetic fields depends only on the gap, but not the mass. If we solve Eq. (2), with  $n = 0$ , for the magnetic field, we obtain

$$\epsilon_g\beta_0^*H_0 = \epsilon_p(\epsilon_p - \epsilon_g). \quad (22)$$

Similarly, from Eqs. (14) and (16), with  $n = 0$ ,  $m = +\frac{1}{2}$ , we have

$$\epsilon_g\beta_0^*H_p = \epsilon_p \left(1 - \frac{\epsilon_p l^2}{\epsilon_p^2}\right) \left[ \epsilon_p \left(1 - \frac{\epsilon_p l^2}{\epsilon_p^2}\right) + \epsilon_g \right]. \quad (23)$$

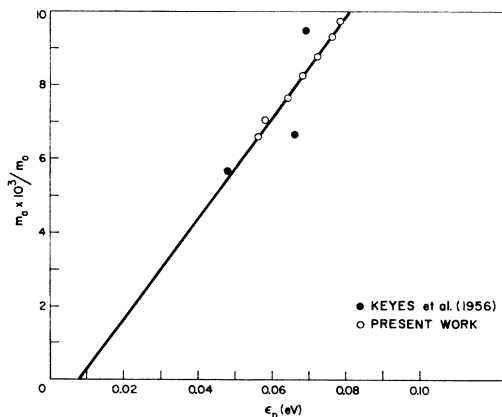

 FIG. 10. Reciprocal periods vs the square of the photon energy with  $H$  along a bisectrix.

The ratio,

$$\frac{H_p}{H_0} = \frac{(1 - \epsilon_p l^2 / \epsilon_p^2)}{(\epsilon_p / \epsilon_g - 1)} \left[ 1 + \frac{\epsilon_p}{\epsilon_g} \left(1 - \frac{\epsilon_p l^2}{\epsilon_p^2}\right) \right], \quad (24)$$

is seen to be independent of  $m_0^*$ , and is, therefore, isotropic. We find that, if we insert our experimental values of  $\epsilon_p$ ,  $H_0$ , and  $H_p$ , and the plasma energy,  $\epsilon_{pl} = 0.0226$  eV ( $55 \mu$ ) of Boyle *et al.*,<sup>15</sup> we obtain  $\epsilon_g = 0.016 \pm 0.001$  eV, in excellent agreement with the value obtained by curve fitting. We have included the plasma line on Fig. 7. Plasma lines were also observed with  $H \parallel$  bisectrix, but the data were too scanty to analyze.

The values of the component masses at the Fermi surface, as deduced by various authors,<sup>5,16</sup> indicate that  $m_2$  is at least a factor of ten larger than any other com-


 FIG. 11. Apparent mass of  $n = 0$  line vs photon energy, for the light mass with  $H$  along a bisectrix.

<sup>15</sup> W. S. Boyle, A. D. Brailsford, and J. K. Galt, Phys. Rev. **109**, 1396 (1958).

<sup>16</sup> Benjamin Lax, Rev. Mod. Phys. **30**, 122 (1958).

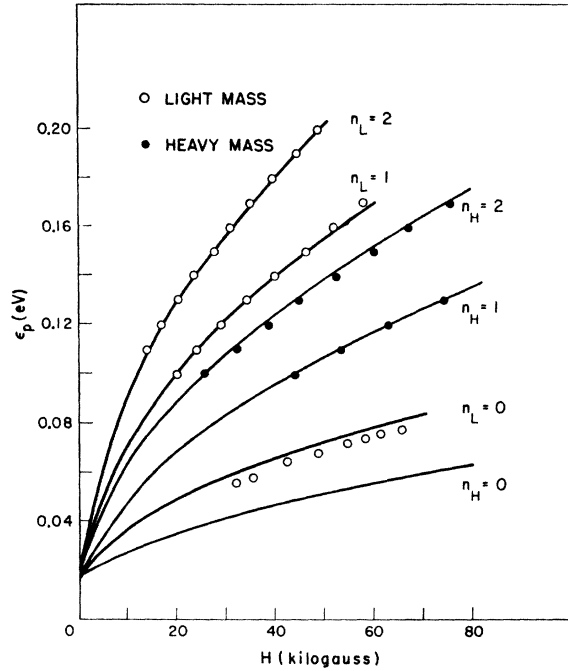


FIG. 12. Photon energies vs magnetic field with  $H$  along a bisectrix. Solid curves are obtained from Eq. (2).

ponent. In this case, Eqs. (17) reduce to

$H \parallel$  binary:

$$\begin{aligned} (m_0^*)_a &= m_0(m_2m_3)^{1/2}, \\ (m_0^*)_b &= (m_0^*)_c = (2/\sqrt{3})m_0(m_1m_3)^{1/2}. \end{aligned}$$

$H \parallel$  bisectrix: (25)

$$\begin{aligned} (m_0^*)_a &= m_0(m_1m_3)^{1/2}, \\ (m_0^*)_b &= 2m_0(m_1m_3)^{1/2}. \end{aligned}$$

There are three small masses, in the ratios  $2/\sqrt{3}:2:1$ , and one relatively large mass. (We have failed to observe this large mass, presumably because the amplitude of the oscillation is reduced by the mass factor.) Reference to Table I shows that our mass ratios are consistent with those of Eq. (25).

From the expression for the cyclotron mass at the Fermi surface (see Appendix),

$$m^* = m_0^*(1 + 2\epsilon_f/\epsilon_g), \quad (26)$$

we may calculate  $\epsilon_f$ , by inserting our values of  $\epsilon_g$  and  $m_0^*$ , and the value of  $m^*$  as measured by Galt *et al.*<sup>17</sup> With  $H$  along a bisectrix axis, we obtain

$$\begin{aligned} \epsilon_f &= \frac{1}{2}[(\epsilon_g/m_0^*)m^* - \epsilon_g] = \frac{1}{2}(7.1 \times 0.0091 - 0.015) \\ &= 0.025 \pm 0.005 \text{ eV}. \end{aligned} \quad (27)$$

The cutoff energies according to Eqs. (12) and (13)

<sup>17</sup> J. K. Galt, W. A. Yager, F. R. Merritt, B. Cetlin, and A. D. Brailsford, *Phys. Rev.* **114**, 1396 (1959); J. E. Aubrey, *J. Phys. Chem. Solids* **19**, 321 (1961).

would then be

$$\epsilon_{p \text{ min}}(n=0) = \epsilon_f + \epsilon_g = 0.040 \text{ eV}, \quad (28)$$

$$\epsilon_{p \text{ min}}(n \gg 1) = 2\epsilon_f + \epsilon_g = 0.065 \text{ eV}. \quad (29)$$

Equation (29) also represents the absorption edge in zero field, and corresponds to a wavelength of  $19 \mu$ , in good agreement with the results of Boyle and Rodgers.<sup>2</sup>

Using these results, we can calculate the de Haas-van Alphen period,

$$\Delta = \epsilon_g \beta_0^* / \epsilon_f (\epsilon_f + \epsilon_g). \quad (30)$$

With the magnetic field in the bisectrix direction, we obtain for the large period,

$$\begin{aligned} \Delta &= 7.1 \times 1.16 \times 10^{-8} / 0.025(0.025 + 0.015) \\ &= 8.2 \times 10^{-5} \text{ G}^{-1}. \end{aligned} \quad (31)$$

This is to be compared with Shoenberg's<sup>11</sup>

$$\Delta = 8.0 \times 10^{-5} \text{ G}^{-1}. \quad (32)$$

Weiner<sup>18</sup> has extended Shoenberg's measurements in bismuth to Bi-Te alloys, and he has compared his results with Cohen's.<sup>7</sup> By making the assumption that, upon alloying with Te, only the Fermi energy changes, he obtains  $\epsilon_g = 0.046 \text{ eV}$ ,  $\epsilon_f = 0.022 \text{ eV}$ . These values are consistent with the transmission edge of Boyle and Rodgers,<sup>2</sup> only if it is an indirect edge occurring at

$$\hbar\omega = \epsilon_f + \epsilon_g = 0.068 \text{ eV} (18 \mu). \quad (33)$$

However, our results indicate a direct edge occurring at

$$\hbar\omega = 2\epsilon_f + \epsilon_g = 0.065 \text{ eV} (19 \mu), \quad (34)$$

and possibly an indirect edge at

$$\hbar\omega = \epsilon_f + \epsilon_g = 0.040 \text{ eV} (31 \mu). \quad (35)$$

We find that our results are not inconsistent with Weiner's measured values. Furthermore, we may, by varying his values within his quoted uncertainties, calculate our value of  $\epsilon_g$  by his method. Since the two values differ by a factor of three, we believe this shows the inaccuracy of his method.

Let us compare our results with the far infrared cyclotron resonance of Boyle and Brailsford.<sup>19</sup> At a wavelength of  $87 \mu$  they obtain a field of 12.8 kG with  $H$  along a binary axis. Inserting this field into Eq. (15), we find  $n=1$ , which we then insert into Eq. (14) with  $m = \frac{1}{2}$ , to obtain  $\epsilon_p = 0.012 \text{ eV}$ , as compared with  $0.014 \text{ eV}$  ( $87 \mu$ ).

We believe that the oscillations seen in transmission by Boyle and Rodgers<sup>2</sup> correspond to the transitions that we have seen in reflection. If this is the case, it is easy to understand why they saw no oscillations at a fixed field as a function of frequency. Their frequency range was severely limited on both ends; on the high end by the transmission edge (which moved to lower fre-

<sup>18</sup> D. Weiner, *Phys. Rev.* **125**, 1226 (1962).

<sup>19</sup> W. S. Boyle and A. D. Brailsford, *Phys. Rev.* **120**, 1943 (1960).

quencies with increasing field), and on the low end by the cutoff energies, given by Eq. (11). The motion of the edge with field is also explained by Eq. (11), which indicates that in a magnetic field transitions having energies smaller than  $2\epsilon_f + \epsilon_g$  are allowed. Furthermore, a plot of their oscillatory data similar to our Fig. 4 yields a period,  $\Delta = 6.8 \times 10^{-5} \text{ G}^{-1}$ , and an intercept close to  $n = -1/2$ . We have included this point on Fig. 5, which shows the agreement with our results.

After having analyzed the present data, it is easy to understand how our previous results<sup>8</sup> led to an incorrect value of the energy gap. The value quoted was  $\epsilon_g = 0.047 \text{ eV}$ . This was obtained by straight line extrapolation to  $H = 0$  of a plot of  $\epsilon_p$  versus  $H$ . We can now show this method to be incorrect. A glance at Fig. 7 may suffice, but it may also be shown that, in the range of observation, the magnetic energy is large compared to the gap, for all transitions except the  $n = 0$  transition, which was not observed previously. On the other hand, it is only when the magnetic energy is small compared to the gap that straight-line extrapolation is valid. Let us choose a point from line *A* in Fig. 2 of reference 8;  $\epsilon_p = 0.088 \text{ eV}$ ,  $H \approx 30 \text{ kG}$ . This line represents the transitions  $(0\downarrow 0\downarrow)$  and  $(1\uparrow 1\uparrow)$ , for which the energy is

$$\epsilon_p = (\epsilon_g^2 + 4\epsilon_g\beta_0^*H)^{1/2}. \quad (36)$$

If we divide by  $\epsilon_g$ , square both sides and insert the values of  $\epsilon_p$  and  $\epsilon_g$ ,

$$1 + \frac{4\beta_0^*H}{\epsilon_g} = \left(\frac{\epsilon_p}{\epsilon_g}\right)^2 = \left(\frac{0.088}{0.015}\right)^2 = 34.5, \quad (37)$$

we see that the magnetic energy is 33.5 times larger than the gap. Furthermore, our previous discussion shows that a reliable value of the gap cannot be obtained without the observation of the  $n = 0$  transition.

#### SUMMARY

Our analysis shows that the Lax model yields a reasonably good fit to the data. Cohen's model is more complex, and allows for (1) a more accurate treatment for the heavy-mass direction, and (2) the possibility of a displacement in  $k$  space of the band edges, depending

on the symmetry of the point in the zone. Our experiment is insensitive to the heavy-mass direction. As far as displaced band edges are concerned, the energy levels involved would be essentially the same, but one would expect different selection rules.<sup>20</sup> It is therefore suggested that this experiment provides evidence for the view that the valence band lies directly beneath the conduction band.

We have found that the energy gap is substantially smaller than the values previously inferred, and we have obtained some of the cyclotron masses at the bottom of the conduction band. We have further shown that the parameter values for the electrons are consistent with the results of cyclotron resonance, de Haas-van Alphen effect, and infrared transmission experiments. In addition, our results indicate that the parameters of the valence band are essentially equal to the electron parameters.

#### ACKNOWLEDGMENTS

The authors wish to express their gratitude to Dr. L. M. Roth for many fruitful discussions, D. F. Kolesar for assistance in carrying out the experiments, J. E. Soares for drawing the figures, and Mrs. S. F. Simon for typing the manuscript. We owe special thanks to the National Magnet Laboratory for the use of the high field magnets throughout these experiments.

#### APPENDIX

In the coordinate system of the principal axes of the energy surface, the cross-sectional area of the Fermi surface normal to the 2 axis is given by<sup>7,21</sup>

$$A(\epsilon_f) = 2\pi(m_1m_3)^{1/2}\epsilon(1 + \epsilon/\epsilon_g)|_{\epsilon=\epsilon_f}. \quad (A1)$$

The cyclotron mass is obtained from this by differentiation,<sup>22</sup>

$$m^*(\epsilon_f) = \frac{1}{2\pi} \frac{dA}{d\epsilon} \Big|_{\epsilon=\epsilon_f} = (m_1m_3)^{1/2} \left(1 + 2\frac{\epsilon_f}{\epsilon_g}\right). \quad (A2)$$

<sup>20</sup> L. M. Roth (private communication).

<sup>21</sup> H. J. Zeiger (private communication).

<sup>22</sup> L. Onsager, *Phil. Mag.* **43**, 1006 (1952).